2012

Molecular mechanisms of K+ selectivity in Na/K pump

Haibo Yu
University of Wollongong, hyu@uow.edu.au

Ian Ratheal
Texas A&M University

Pablo Artigas
Texas A&M University

Benoit Roux
University of Chicago

Molecular mechanisms of K+ selectivity in Na/K pump

Abstract

The sodium–potassium (Na/K) pump plays an essential role in maintaining cell volume and secondary active transport of other solutes by establishing the Na^+ and K^+ concentration gradients across the plasma membrane of animal cells. The recently determined crystal structures of the Na/K pump to atomic resolution provide a new impetus to investigate molecular determinants governing the binding of Na^+ and K^+ ions and conformational transitions during the functional cycle. The pump cycle is generally described by the alternating access mechanism, in which the pump toggles between different conformational states, where ions can bind from either the intracellular or the extracellular side. However, important issues concerning the selectivity of the Na/K pump remain to be addressed. In particular, two out of the three binding sites are shared between Na^+ and K^+ and it is not clear how the protein is able to select K^+ over Na^+ when it is in the outwardly facing phosphorylated conformation (E2P), and Na^+ over K^+ when it is in the inwardly facing conformation (E1). In this review article, we will first briefly review the recent advancement in understanding the microscopic mechanism of K^+ selectivity in the Na/K pump at the E2.Pi state and then outline the remaining challenges to be addressed about ion selectivity.

Keywords

na, pump, selectivity, molecular, k, mechanisms, CMMB

Disciplines

Life Sciences | Physical Sciences and Mathematics | Social and Behavioral Sciences

Publication Details

Yu, H., Ratheal, I., Artigas, P. & Roux, B. (2012). Molecular mechanisms of K+ selectivity in Na/K pump. Australian Journal of Chemistry: an international journal for chemical science, 65 (5), 448-456.

Molecular mechanisms of K^+ selectivity in Na/K pump

Haibo Yu[1,*], Ian Ratheal[2], Pablo Artigas[2], Benoît Roux[3]

[1]School of Chemistry, University of Wollongong, NSW 2522, Australia [2]Department of Cell Physiology and Molecular Biophysics, Texas Tech Health Sciences Center, Lubbock, Texas, USA [3]Department of Biochemistry and Molecular Biology, University of Chicago, Chicago, IL, USA

*Correspondance author: hyu@uow.edu.au

For submission to Australian Journal of Chemistry

Abstract

The sodium/potassium pump (Na/K pump) plays an essential role in maintaining cell volume and secondary active transport of other solutes by establishing the Na^+ and K^+ concentration gradients across the plasma membrane of animal cells. The recently determined crystal structures of the Na/K pump to atomic resolution provide a new impetus to investigate molecular determinants governing the binding of Na^+ and K^+ ions and conformational transitions during the functional cycle. The pump cycle is generally described by the alternating access mechanism, in which the pump toggles between different conformational states, where ions can bind from either the intracellular or the extracellular side. However, important issues concerning the selectivity of the Na/K pump remain to be addressed. In particular, 2 out of the 3 binding sites are shared between Na^+ and K^+ and it is not clear how the protein is able to select K^+ over Na^+ when it is in the outwardly facing phosphorylated

conformation (E2P), and Na^+ over K^+ when it is in the inwardly facing conformation (E1). In this review article, we will first briefly review the recent advancement in understanding the microscopic mechanism of K^+ selectivity in the Na/K pump at the E2•Pi state and then outline the remaining challenges to be addressed about ion selectivity.

Keywords: sodium-potassium pump, P-type ATPase, ion selectivity, molecular simulations, electrophysiology, protonation states, pH effects

Introduction

Ion channels and pumps are fascinating biological molecular-scale nano-machineries. They mediate the transport of diverse ions across membranes either passively or actively and thus play an important role for normal cell functions. Malfunction of these channels and pumps often causes in the development of pathophysiological conditions. Therefore, they are recognised as important therapeutic targets for treating a wide range of diseases. Among them, the sodium-potassium pump (Na/K pump), one of the first membrane proteins characterised[1,2], is a large heterodimeric membrane-bound proteins compromising a catalytic α-subunit (~1,000 residues, ~105kDa) and a heavily glycosylated β-subunit (~300 residues, ~55 kDa). Na/K pump is energized by ATP hydrolysis and belongs to the P-type ATPase family because a transient phosphorylated intermediate is formed at a conserved Asp residue during catalysis[3]. For each ATP that is hydrolysed, the Na/K pump moves three Na^+ ions out of and two K^+ ions into the cell by alternating two different conformations, E1 and E2, according to the "alternative access" scheme[4,5] (Figure 1). Under physiological conditions, the extracellular-facing state E2P preferentially binds two K^+ in the presence of a 30-fold greater external concentration of Na^+ ions, whereas the cytoplasmic-facing state E1 selects three Na^+ in the presence of a 10-fold higher internal concentration of K^+ ions. Due to this imbalance in cation exchange and the activity of ion-specific channels, an electrical gradient across the plasma

membrane is generated and maintained. These combined electrochemical gradients are crucial for many basic and specialized cellular functions in animal cells, such as generation of the action potentials responsible for excitability, secondary active transport of nutrients and other molecules across the plasma membrane, signaling and volume regulation. The Na/K pump is the therapeutic target of digitalis (such as digoxin), which have been used in the treatment of congestive heart failure for centuries[6].

Very recently, new information on the structure and function of the Na/K pump has emerged from high-resolution X-ray crystal structures[7,8]. In 2007, Morth et al. reported the first crystal structure of the Na/K pump from pig (resolution 3.5 Å, PDB id: 3B8E)[9] and in 2009, Toyoshima's group published another crystal structure of Na/K pump from shark with a 2.4 Å resolution (PDB id: 2ZXE)[10]. Previous studies have established that there are three distinct cation-binding sites involved in the functional pumping cycle (Figure 1). Of the three ion-binding sites, Sites I and II can bind either Na^+ or K^+ depending on the functional state thus they are called shared sites, but Site III exclusively binds Na^+ at the E1 state. Both crystal structures captured the so-called E2•P_i state, revealing how the two K^+ ions are coordinated at the shared sites I and II between transmembrane helices (TM) 4, 5 and 6. It has been postulated that sites I and II will rearrange to coordinate two Na^+ ions, whereas other residues in TM 5, 8 and 9 have been proposed to bind the third Na^+ ion at the E1 state (Site III)[11]. How the Na/K pump is able to achieve such variations in ion selectivities with the same shared binding sites is a very intriguing question that has not, so far, been answered. Recently, we have been using computations based on atomic models together with electrophysiological experiments to shed some new light on the physiochemical principles underlying the ion selectivity of the Na/K pump.

This review article is based on the talk presented at BioPhysChem2011 - the joint RACI Physical Chemistry Division and Australian Society for Biophysics annual meeting - held at

Wollongong, Australia in Dec 2011. In this article, we will briefly review recent work on the molecular mechanism of ion selectivity in Na/K pump, including two of our papers[12,13] and then outline the outstanding questions that remain to be addressed. Readers are referred to Ref. [12,13] and references therein for more details.

Protonation States of Key Acidic Residues in the K^+ Binding Sites

Both Na/K pump crystal structures reveal that the K^+ binding sites at the E2•P_i state superimpose surprisingly well with the binding sites of the sarcoplasmic reticulum Ca^{2+} pump (SERCA) in the corresponding Ca^{2+}-free state[9,10]. The occluded K^+ ions are well coordinated by acidic and polar side-chains and some main-chain carbonyls. Four particularly important residues contributing acidic side-chains are in direct contact with the cations: Glu334, Glu786, Asp811 and Asp815 (the shark Na/K pump numbering was adopted throughout the text). This observation poses an intriguing question as to how these different pumps can recognize and transport two different ions (K^+ for Na/K pump or H^+ for SERCA) with the very similar binding sites. Additionally, how these negatively charged binding sites in the Na/K pump at the E2•P_i state achieve the required K^+ over Na^+ selectivity is not well understood. Vrbka et al. have shown with both quantum mechanics and classical molecular dynamics simulations that the negatively charged species such as formate and acetate prefer Na^+ over the slightly larger K^+ in aqueous solution with a selectivity of ~2 kcal/mol. This has been used to rationalize the higher affinity of Na^+ over K^+ to protein surfaces[14]. Furthermore, statistical analyses of the high-resolution crystal structures deposited in the PDB show that the average number of charged functional groups in the Na^+ binding site is ~1.12, in contrast to ~0.70 in the K^+ binding sites[15]. These two pieces of evidence seem to be incompatible with the fact the crystallographically resolved structures are capable of achieving the K^+ selectivity with the binding sites formed with four residues expected to bear negative charges. Interestingly, equilibrium molecular dynamics simulations with these four titratable residues deprotonated

lead to a large distortion of the binding sites (Figure 2B) and thermodynamically, the binding sites become Na^+ selectively (Table 2 Simulation A, see below for detailed discussion). The large structural deviation from X-ray structures can be explained by the very short distance between the two negatively charged residues Glu786 and Asp811 in close contact with each other (the shortest distance between the oxygen atoms: 2.7 Å in 3B8E and 2.8 Å in 2ZXE), which will result in strong electrostatic repulsions. It is worth recalling that at the 2.4 Å resolution of the X-ray structure, hydrogen atoms cannot be detected. This motivated us to carry out pKa calculations for these titratable residues to predict their protonation states under physiological conditions (Table 1). Our pKa calculations predict that Asp811 is deprotonated while Asp815, Glu334 and Glu786 are protonated. With these acidic residues adopting the predicted protonation states, the binding sites are stable in the equilibrium simulations with a room mean square deviation (RMSD) for the heavy atoms around 0.5-1.0 Å (Figure 2A). During the simulations, the protonated Glu786 and the deprotonated Asp811 form a so-called strong di-acid hydrogen bond to help stabilize the binding sites[16]. In reality, this shared proton will be delocalized if they were described with quantum mechanics instead of classical molecular mechanics models applied in the current study[17]. We would like to note that the calculated protonation states for all the key acidic residues are in broad agreement with previous data obtained for the homologous residues of SERCA in the corresponding functional state[18-20] (see below for more discussions).

Ion Selectivities in the Na/K pump at the E2·Pi State

Thermodynamically, the ion selectivity at the binding sites is defined as $\Delta\Delta G_{\mathrm{Na,K}} = \left[G^{\mathrm{site}}_{\mathrm{Na}} - G^{\mathrm{bulk}}_{\mathrm{Na}}\right] - \left[G^{\mathrm{site}}_{\mathrm{K}} - G^{\mathrm{bulk}}_{\mathrm{K}}\right] = \Delta G^{\mathrm{site}}_{\mathrm{Na,K}} - \Delta G^{\mathrm{bulk}}_{\mathrm{Na,K}}$, where $\Delta G^{\mathrm{site}}_{\mathrm{Na,K}} = \left[G^{\mathrm{site}}_{\mathrm{Na}} - G^{\mathrm{site}}_{\mathrm{K}}\right]$ and $\Delta G^{\mathrm{bulk}}_{\mathrm{Na,K}} = \left[G^{\mathrm{bulk}}_{\mathrm{Na}} - G^{\mathrm{bulk}}_{\mathrm{K}}\right]$. By this definition, a binding site is K^+ selective when $\Delta\Delta G_{\mathrm{Na,K}}$ is positive

and Na^+ selective when $\Delta\Delta G_{Na,K}$ is negative. The free energy difference between Na^+ and K^+ in bulk water, $\Delta G^{bulk}_{Na,K} = \left[G^{bulk}_{Na} - G^{bulk}_{K}\right]$, is about ~ -17.5 kcal/mol[21]. All-atom alchemical free energy perturbation molecular dynamics simulations (FEP/MD) can be carried out to compute $\Delta G^{site}_{Na,K} = \left[G^{site}_{Na} - G^{site}_{K}\right]$, the relative free energy difference between K^+ and Na^+ at the cation binding sites. Such a theoretical approach is based on the assumption that ion selectivity in the Na/K pump can be understood on the basis of thermodynamic binding equilibrium, leaving out kinetic considerations (see below). The FEP/MD simulations showed that the shared cation binding sites (Site I and II) at the E2•P_i state are indeed K^+ selective (Table 2 Simulation B) when the key acidic residues adopt the predicted protonation states (i.e. Asp811 deprotonated and Glu334, Glu786 and Asp815 protonated). The calculated relative free energies compare well with available experimental estimates[22].

Of particular interest, the calculated relative free energies for K^+ to Na^+, $\Delta\Delta G_{Na,K}$, reveal that ion selectivity is extremely sensitive to the protonation states of those four acidic side chains. When all four acidic residues are deprotonated, a large distortion from the X-ray structure (Figure 1B) was observed and the binding of Na^+ over K^+ to sites I and II is considerably more favorable (Table 2 Simulation A). Additional FEP/MD calculations have been carried out to investigate the effects of protonation states of residues Glu334 (Table 2 Simulation C), Glu786 (Table 2 Simulation D) and Asp815 (Table 2 Simulation E). In all three cases, substantial selectivities for K^+ are compromised when any of these residues becomes deprotonated. This reinforces the conclusion from pKa calculations that those acidic side chains must be protonated to yield structural stable K^+ selective binding sites in the Na/K pump at the E2•P_i state.

Impact of External pH on K^+ Selectivity

The suggestions that protonation of acidic side chains involved in the shared binding sites I and II are specifically implicated in the selectivity of the cation binding sites of the Na/K pump is both novel and provocative. The computational analyses predict that the K^+ selectivity at the shared sites will be affected by extracellular pH. Increasing the extracellular pH should increase the probability of deprotonation of the key acidic residues and thus undermine the ability of the shared sites to select K^+ over Na^+ (Table 2 Simulations A, C, D, and E). To experimentally test this prediction, two-electrode voltage clamp experiments were performed to study the function of the Na/K pump expressed in *Xenopus* oocytes at different extracellular pHs. Physiologically, the outward-facing state that selects K^+ over Na^+ is actually E2P, that is, the state that precedes E2·Pi in the forward pump cycle (Figure 1). All the calculations, in contrast, are based on the E2·Pi state captured by the crystal structures, though both states are expected to select K^+ over Na^+ with a similar mechanism.

To evaluate the impact of external pH on K^+ selectivity, we measured the concentration of extracellular K^+ that half-maximally activates the Na/K pump current ($K_{0.5}$) at pHs 7.6 and 9.6 (Figure 3). Figure 3A shows results of a titration experiment performed in an oocyte bathed by 125 mM external Na^+. From these measurements, we can fit the Hill equation as a function of extracellular K^+ concentration to extract the dissociation constant $K_{0.5}$ at each voltage. Figure 3B summarises that the results in several oocytes either in the presence (filled symbols) or absence of external Na^+ (open symbols, Na^+ was replaced with the inert cation N-methyl-D-glucamine (NMG)). A reduction in the apparent affinity (inverse of $K_{0.5}$) for external K+ was observed in both cases when the external pH was increased, indicating that an increase in pH impaired the ability of K^+ to compete with Na^+ for the shared sites. $K_{0.5}$ was smaller in the absence of external Na^+ than in its presence owing to the lack of competition from Na^+. The apparent affinity for external K^+ at positive voltages in the presence of Na^+ was reduced to about 25-30% when the external pH was increased from 7.6 to 9.6 (filled symbols). This

corresponds to an effective free energy change in $\Delta\Delta G_{Na,K}$ of ~ -0.8 kcal/mol (i.e. the K^+ selectivity decreases by the amount of 0.8 kcal/mol). This observation can be rationalised that the probability of the protonated state of the carboxylate side chains decreases slightly when the binding sites are exposed to high extracellular pH in the outwardly open state, resulting in a small decrease in the apparent K^+ selectivity.

Both sets of experiments demonstrate that external K^+ competes less well with external Na^+ for the shared sites I and II when the extracellular pH is increased, as predicted by our computations. This observation is also consistent with previous studies[23-27]. It was noted as early as 1980s by Skou and co-workers[24] that the abundant extracellular protons increase the apparent affinity for K^+ and a decrease in protons increased the apparent affinity for Na^+. However, to the best of our knowledge, all the previous studies have attributed such a pH-dependence phenomenon to either the relative stability of the E1 and E2 conformational states or the concentrations of ions at the access channel at different pHs[27]. Although the current available data cannot rule out such a rationalisation, our computational and electrophysiological studies suggest a more direct effect of extracellular pH on the electrostatic environment of the cation binding sites by modulating the protonation states of key acidic residues.

The Flexibility of the Cation Binding Sites

In the equilibrium simulations, it is observed that the acidic side chains have a root-mean-square fluctuation (RMSF) in the order of 0.5 to 1.0 Å. This atomic positional fluctuation is larger than the atomic radii difference between Na^+ and K^+ (~0.38 Å)[28]. This challenges the so-called classical "snug-fit" mechanism in the field of permeation and ion channels[29], solely relying on the ability of the binding site to retain its local conformation very precisely to provide a good geometric fit for K^+, but not for the slightly smaller Na^+[28,30]. Furthermore, it has been

shown that external K^+ can be substituted equally well with other monovalent metal ions (e.g. Li^+ and Cs^+) and even organic cations of much larger size (e.g. formamidinium$^+$ (Form) and acetamidium$^+$ (Acet)) in the Na/K pump expressed in *Xenopus* oocytes[13] (Figure 4B). Most surprisingly, Form and Acet can act as external K^+ surrogates and induce K^+-like outward currents in the Na/K pump cycle (~70% or ~80%, respectively, of K^+ induced outward currents, Figure 3B in Ref. [13] and Figure 4). The large outward currents observed with Form/Acet suggest that two organic ions, in replacement for K^+, might be exchanged for three Na^+ ions, thus preserving the normal 3:2 stoichiometry of the pump. These observations motivated us to carry out molecular dynamics simulations of the putative occluded states with two bound Acet in order to structurally rationalise the experimental results. A series of configurations were generated with two Acet molecules docked into the K^+ sites of the X-ray structure 2ZXE with random orientations. One plausible orientation was chosen arbitrarily to perform 20 ns MD simulations to assess the magnitude of structural distortion induced by the organic cation within the binding sites. Figure 4C shows the final snapshots after simulations, compared with the corresponding structure with two bound K^+ ions after a comparable 20ns MD simulation (Figure 4D). The RMSD of nonhydrogen atoms of the key residues participating in the coordination average from the MD trajectories is on the order of 1.5 Å, showing that the binding sites are minimally disturbed by the bound organic cations. Similar interaction patterns were observed in the Acet occluded and K^+ occluded states. We conclude that the shared binding sites I and II in the Na/K pump is relatively flexible and it can adapt to accommodate larger organic ions (e.g. Form and Acet). This view is also in broad accord with previous studies of ion selectivities for other membrane proteins[15,28,30-32].

Effects of Site-directed Mutagenesis

The conclusion that in the E2·Pi state, Glu334, Glu786 and Asp815 are protonated and neutral while Asp811 is deprotonated and negatively charged suggests that the K^+ over Na^+ selectivity

should be strongly perturbed by the mutation D811N, but not by the charge-conserving mutations E334Q, E786Q and D815N. This is qualitatively consistent with previous mutagenesis studies reported in the literature, although the quantitative effects of such mutants may be complicated by possible major changes in conformational equilibrium that we cannot address in this type of calculations. The mutants E334Q[33] and E786Q[34] are able to transport K^+. In contrast, the D811N mutant is severely impaired and produces no pump currents[34]. The mutant D815N presents complex functional effects. Nevertheless, it is reported both the neutralising D815N mutant the charge conservative mutant D815E have a reduced K^+ apparent affinity[34].

We also carried out the FEP/MD simulations to study the effects of site-directed mutagenesis at the key acidic residues on the K^+ over Na^+ selectivity (Table 2, Simulation F, G and H) in isolation from other major functiona effects. The snapshots at the end of 10 ns equilibrium simulations for the mutants are compared with the crystal structure (Figure 5). In the D815N mutant (Table 2 Simulation F), the effects introduced by the mutation on K^+ selectivity is rather limited. This might be due to the fact that the carboxylate oxygens do not participate in direct coordination of Site I (Figure 5A) and that the perturbation introduced by D815N is rather small compared to the wild-type simulation (Table 2 Simulation B) and the X-ray structure (2ZXE). In the E334Q (simulation G) and E786Q (simulation H), the K^+ selectivity at both Sites I and II are considerably lost or become slightly Na^+ selective. As observed Figure 5B and C, the distortions introduced by the E334Q and E786Q are much more visible. It is worth pointing out that such FEP/MD based ion selectivity calculations do not provide any information on the apparent affinity instead reportes the relative free energy difference between K^+ and Na^+, thus comparison with experimental data is not always straightforward. Furthuremore, rigorously speaking, the neutralising mutation is not structurally equivalent to protonation, which complicates direct comparison.

Comparison with SERCA

Structural understanding of the Na/K pump mechanism is rather limited because few crystal structures are available. No structures of the crucial E1 state have been published to date. In comparison, more than 20 crystal structures that span more than 10 functional states have been reported for SERCA[35]. Even though the overall sequence similarity between the Na/K pump and SERCA is relatively low (~30%), the 3D structural topology adopted by them is very similar and the cytoplasmic domains and the ten transmembrane helices (TM1-TM10) are superimposable[9,10]. The structural resemblance of the cation binding pocket of the Na/K pump to the SERCA pump is surprising highly[9-11]. Although SERCA transports Ca^{2+} and H^{+} whereas the Na/K pump transports Na^{+} and K^{+}, considering the high similarity between the mechanisms of functions (Figure 1) and the cation binding site residues, comparison between these two pumps can help elucidate the molecular mechanism for the Na/K pump especially in the scenarios where little is known.

The side-chain protonation and mobility of the cation binding sites in SERCA have been studied in the literature with a diverse set of techniques including pKa calculations, Fourier transform infrared (FTIR) spectroscopy, and molecular dynamics simulations. These collectively provide a direct comparison with our recent work. Several groups have carried out pKa calculations on the key acidic residues of the cation binding sites of SERCA at the Ca^{2+}-free state[18-20,36]. Due to the inherent limitations for these continuum electrostatics or empirical function based pKa calculation methods, there is some inconsistency in assigning the exact protonation states for those acidic residues with a pKa around 7. Nevertheless, it is generally agreed that some of four acidic residues must be protonated at the Ca^{2+}-free state. The pKa values for the homologous residues of the Na/K pump and SERCA at the E2·Pi state are in broad agreement (Table 1). The involvement of protonation and deprotonation of these residues during the functional cycle of SERCA was further probed experimentally by FTIR. The

pH dependence of infrared bands in the FTIR difference spectra from the E1 state to the E2 state has been assigned to the vibrational signature from the C=O double bonds due to protonation of acidic side chains[36,37]. This provided first direct evidence for the protonation of carboxyl groups upon Ca^{2+} release reaching the E2·Pi state and it was concluded that these acidic residues are primary candidates for the proton countertransporting residues for SERCA. Very recently, the effects of the protonation states of these residues on the stability of the cation binding sites in SERCA were systematically investigated with long time molecular dynamics simulations. Eight different combinations of the protonation of four acidic residues, Glu309, Glu771, Asp800 and Glu908 (SERCA numbering), were tested. It is found that only Asp800 as charged is most likely at the E2·Pi state and protonation of the three other acidic residues plays an important role in stabilising the binding pocket[38]. These three lines of evidence (pKa calculations, FTIR and molecular dynamics simulations) ubiquitously indicate that three out of four acidic residues in SERCA are likely to be protonated at the E2·Pi state. These data further support the proposed protonation scheme for the Na/K pump at the E2·Pi state: Glu334, Glu786 and Asp815 are mostly likely protonated and Asp811 is deprotonated under physiological conditions[12].

One the other hand, the high similarity for the cation binding sites between SERCA and the Na/K pump also raises a fundamental question: Why is the Na/K pump able to bind K^+ and many other monovalent cations, including organic ions, whereas SERCA binds only H^+ at the E2 state? Based on the X-ray structures, it has been argued that even slight rearrangement in the side chain orientation might be sufficient to modulate the ion selectivity of the different states of the Na/K pump[39]. It might be expected that the subtle difference between SERCA and the Na/K pump might contribute to the different ion selectivities[8]. To fully understand different ion selectivities in the P-type ATPase, further work, both computational and experimental, will be required.

Possible Proton Source and Sink

According to our computational studies, protonation of Glu334, Glu786 and Asp815 is absolutely required establish the robust K+ selectivity at the shared binding sites in the Na/K pump[12]. Additionally, a recent study by Poulsen et al. concluded from a joint electrophysiology and molecular dynamics simulation study that two additional cytoplasmic protons enter and stabilise the vacant site III by protonating Asp933 and Glu961 at the E2 state, and return to the cytoplasm via a transient aqueous pathway when the K^+ ions are released in the E1 state[40]. Altogether, there will be at least five protons explicitly involved in the E2 state. On the other hand, it is known that during the functional cycle there is only net transport of Na^+ and K^+, i.e. the Na/K pump does not actively pump protons. This imposes strict constraints on the possible source and sink for the protons implicated in any proposed mechanism including the one proposed here[12]. In close correspondence with the mechanism proposed in Ref. [40] Figure 4, one possibility is that all these protons come from and return to the cytoplasmic side to maintain the asymmetric stoichiometry. As a result, the binding sites I, II and III composed of the deprotonated carboxylates (including Glu334, Glu786, Asp811, Asp815, Asp933 and Glu961) will produce a robust Na^+ over K^+ selectivity at the E1 state[28]. But alternative mechanisms are conceivable. For example, some of the acidic residues coordinating the ions might remain protonated at the E1 state and only a subset of protons undergoes such transient movements during the pumping cycle. The presence of a few protonated carboxylates at the cation binding sites does not necessarily mean that the binding site is unable to achieve Na^+ selectivity, as indicated by FEP/MD simulations based on simplified reduced models[41]. Taking together, these two studies suggest the hypothesis that the Na/K pump might control the chemistry of ion coordination by modulating the protonation states of key residues forming the cation binding sites to achieve the K^+ and Na^+ selectivities required at various stages of the functional cycle[12,40]. To fully understand the microscopic mechanism of

ion selectivity at the shared binding sites and the exclusive Na^+ binding sites, it is crucial to obtain more structural information about the E1 state.

Summary and Outlook

It may not be surprising that the underlying mechanism of ion selectivity in the Na/K pump is considerably more complex than the mechanisms observed in ion channels since the latter are required to support a single type of ion selectivity as they function. The combined results from our computations and experiments show that the protonation states of key acidic residues have both structural and energetic impacts on the function of the Na/K pump at the E2·Pi state. We demonstrated that protonation of Glu334, Glu786 and Asp815 is absolutely required both to ensure the structural integrity of binding sites I and II of the Na/K pump in the K^+-loaded E2·Pi state, and to establish the robust selectivity of those sites for K^+ over Na^+. Although the present study was concerned exclusively with the K^+ selectivity of the E2·Pi and E2P states, these findings beg the question of whether the same physiochemical factors have a corresponding role in establishing the Na^+ selectivity at the E1 state. However, without high-resolution X-ray structures of the Na^+-loaded E1 state, it is difficult to definitively determine the molecular basis for the Na^+ selectivity. Further work will be required to resolve these issues.

In our current study, we adopt the simplest view of conductive-state selectivity starts with the assumption that there exist well-defined cation binding sites that can be occupied by either K^+ or/and Na^+, which might be a reasonable approximation for ion pumps since it has to first bind the specific ions before conducting them. But conductive-state selectivity can be also a result of kinetic factors caused by free energy barriers[42,43]. Furthermore, it is good to recall that ion pumps are not designed to keep ions bound in place, but to transport them across membrane. Thus, a more complete understanding of conductive-state selectivity requires the knowledge of the entire free energy surface governing the whole functional cycle, with all its free energy

wells and barriers determined. To fully characterise the free energy landscape with atomic details, more detailed structural view of the Na/K pump, in particular, at the E1 state and the conformational transitions between different functional states is desperately needed.

It is worth emphasising that any conclusions derived from computational studies of ion selectivity depend on the accuracy of underlying computational methods and molecular models[44,45], both of which are currently under active development. Most of the computational studies of ion channels and pumps are based on the non-polarisable force fields, in which the polarisation effects are treated in a mean-filed manner[46-48]. However, the inherent limitations of such force fields might prevent it from providing a quantitative description of ion selectivity in biological channels and pumps due to lack of charge transfer and induced polarisation effects[49-52]. One particular advancement in the field worth noticing is the development of potential functions that explicitly account for induced polarisation, which has shown improved description of electrostatics interactions in heterogeneous environment[53-58]. On the other hand, combined quantum mechanics and molecular mechanics (QM/MM) methods have been applied to investigate the coordination properties in potassium channels[50], however, due to the dramatically increased computational costs, the thermodynamic properties of ion selectivities have not been characterised yet with combined QM/MM simulations. Nevertheless, with the development of advanced computational models and the continuing progress of computing power, it is expected that computer simulations will shed more light on the mechanisms of ion selectivities in ion pumps.

To summarise, with joining forces with experimental techniques and computational studies, research into understanding the molecular mechanism of the Na/K pump will continue to advance and further studies will provide us with detailed mechanistic view about their functions.

ACKNOWLEDGMENT: H.Y. is grateful to Dr Ron Clarke (University of Sydney) and Prof Andreas Barth (Stockholm University, Sweden) for insightful discussions. We thank Prof Christopher Rowley (Memorial University of Newfoundland, Canada) for critical reading of the manuscript. The work was in part supported by US National Institute of Health Grant GM062342 (H.Y. and B.R.), by American Heart Association Grant BGIA2140172 (P.A.) and by the University of Wollongong URC Small Grant Scheme (H.Y.). H.Y. is an Australian Research Council Future Fellow (FT110100034).

Table 1: The predicted pKa values and protonation states of binding sites residues of the Na/K pump and SERCA at the E2•P_i state.

	NaK Pump PDB id: 3B8E[9]			NaK Pump PDB id: 2ZXE[10]				SERCA PDB id: 1WPG[20]		Predicted Protonation States
Methods	MCCE ε_p=4.0	MCCE ε_p=8.0	PROPKA	MCCE ε_p=4.0	MCCE ε_p=8.0	PROPKA	FEP/MD		MCCE ε_p=4.0	
Asp811	2.6	4.2	0.9	1.0	2.8	3.7	-	Asp800	7.1	Protonated
Asp815	13.1	8.3	6.8	3.0	3.8	5.8	9.4 (10.8)	Glu908	>14	Deprotonated
Glu334	>14	12.3	10.9	13.8	8.4	8.3	-	Glu309	8.4	Protonated
Glu786	12.9	9.1	9.8	>14	>14	10.7	-	Glu771	>14	Protonated

pKa was calculated from the Poisson-Boltzmann equation with Multiple Conformation Continuum Electrostatics (MCCE)[59,60], the empirical method PROPKA 3.0[61] and free energy perturbation method based on the explicit solvent free energy perturbation molecular dynamics simulations (FEP/MD). The corresponding values for the Ca^{2+} pump in the E2•P_i state were taken from Ref. [20] . The K^+ ions were included in all the pKa calculations. Two different values of the protein dielectric constant (ε_p=4.0 and 8.0) were used to investigate the sensitivity to this parameter. The pKa shift of Asp815 was also calculated with explicit solvent using a FEP/MD with or without a combined umbrella sampling potential of mean force method (in parenthesis). See Supplementary Information in Ref. [12] for more details.

Table 2: FEP/MD calculations for the cation binding sites I and II in the wild-type and mutant Na/K pump at the E2·P_i state.

Simulations	Key Acidic Residues at the Cation Binding Sites I and II				$\Delta\Delta G_{Na,K}$ (kcal/mol)	
					Site I	Site II
A	E334-	E786-	D811-	D815-	-2.5(-1.7)	-2.7(-4.5)
B	E334	E786	D811-	D815	+1.9(+3.0)	+4.0(+1.7)
C	E334	E786	D811-	D815-	-1.5	+3.5
D	E334-	E786	D811-	D815	-1.2	-7.7
E	E334	E786-	D811-	D815	-2.9	-3.0
F	E334	E786	D811-	D815N	+3.1	+6.3
G	E334Q	E786	D811-	D815	+0.3	+0.0
H	E334	E786Q	D811-	D815	-0.2	+1.0

Minus symbol "-" denotes deprotonation of the acidic residue (i.e. negatively charged). Unless specified otherwise, all calculations are based on the crystal structure PDB id: 2ZXE[10]; Results based on the structure PDB 3B8E[9] are given in parentheses for comparison. The simulations of mutants (F, G and H) were constructed *in silico* based on the well-equilibrated wild-type configurations (see Supplementary Information in Ref. [12] for more details).

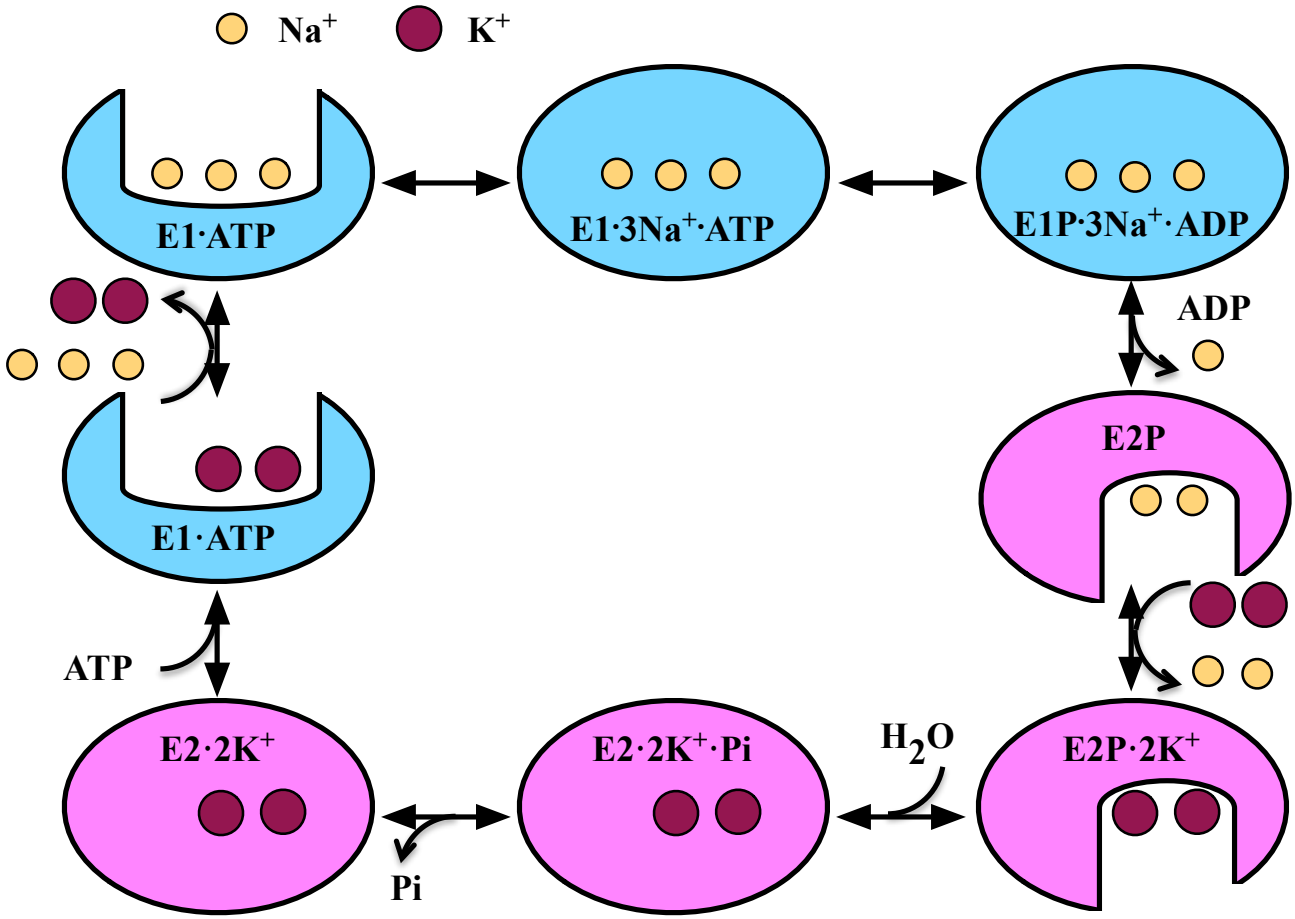

Figure 1: The functional cycle of the Na/K pump[4,5,7,8]. Binding of Na^+ to the E1·ATP state from intracellular space induce phosphorylation, leading to the formation of the Na^+ occluded E1P·3Na^+·ADP state and a subsequence conformational transition to the E2P state. The E2P state has a lower affinity for Na^+, leading to exchange of three Na^+ for two K^+ from the extracellular space. Closure of the E2P state leads to E2P dephosphorylation and formation of the K^+ occluded E2·2K^+·Pi state (two crystal structures were determined for this state, PDB id: 3B8E[9] and 2ZXE[10]). ATP binding leads to the formation of the E1 state and consequent release of K^+ into the intracellular space and binding of Na^+.

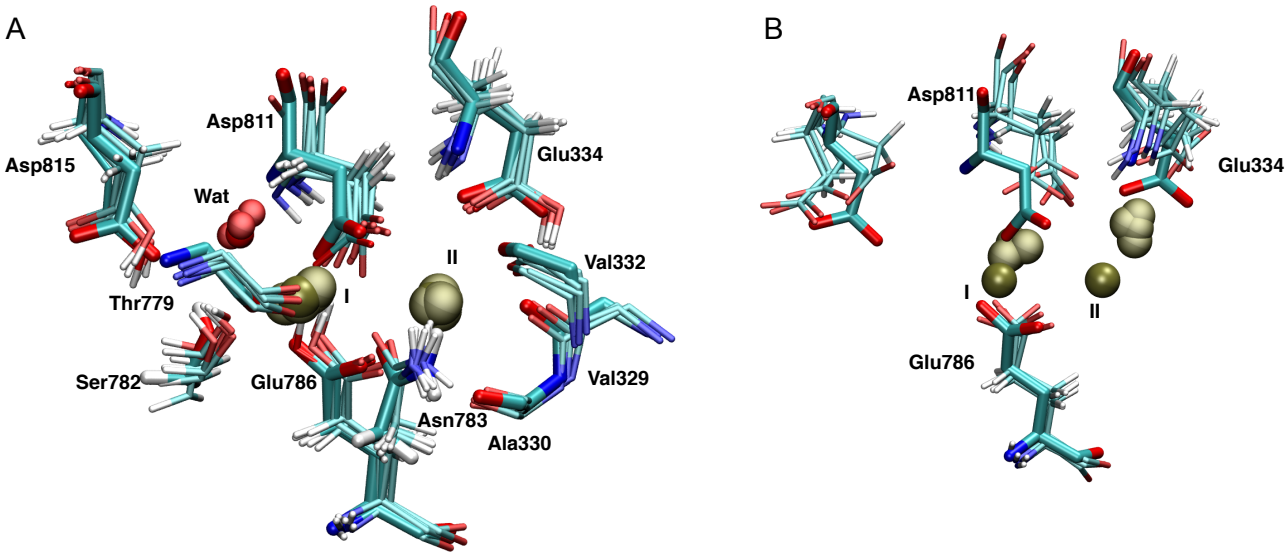

Figure 2: Superposition of the X-ray structure and snapshots from the simulations based on the crystal structure 2ZXE (drawn with thicker lines and ions darker). A. Snapshots taken at 5ns, 8ns, 11ns, 14ns, 17ns, and 20ns with the protonation states of the binding site residues assigned according to the theoretical prediction (Table 1); the average heavy-atom RMSDs are (in Å) 0.5 for Glu334, 0.4 for Glu786, 0.8 for Asp811, and 0.8 for Asp815. B. Snapshots taken at 5ns, 6ns, 7ns, 8ns, 9ns, and 10ns with the binding site residues deprotonated; The average heavy-atom RMSD are (in Å) 1.7 for Glu334, 1.0 for Glu786, 2.2 for Asp811, and 1.5 for Asp815. Figure was adapted from Ref. [12].

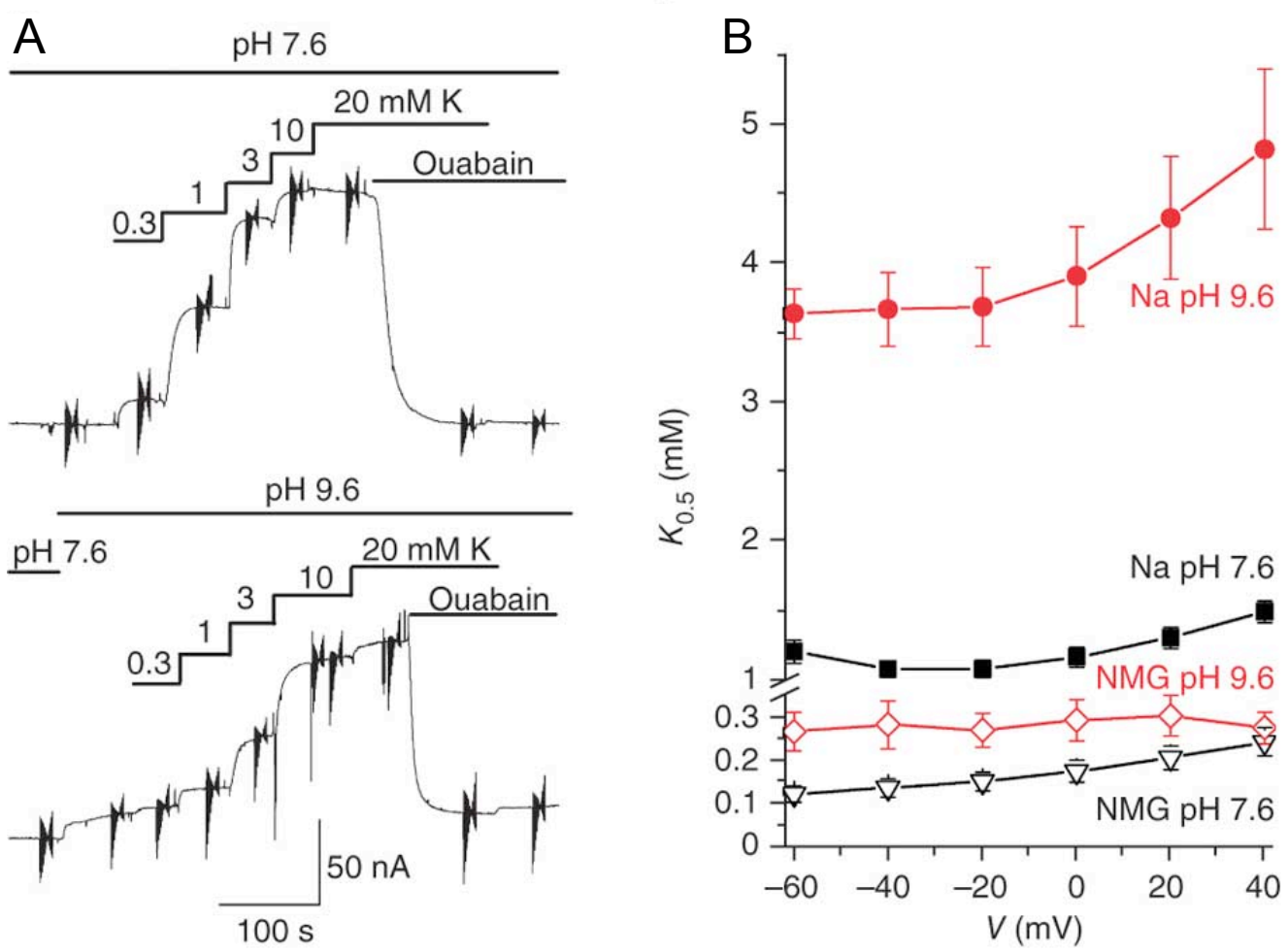

Figure 3: Electrophysiological experiments on the Na/K pump expressed in *Xenopus* oocytes at different extraceullar pHs. A. K^+-induced mediated outward pump currents from a single Na^+-loaded oocyte held at -50 mV in the presence of 125 mM Na^+ at two different external pHs (top, 7.6; bottom, 9.6). Vertical deflections of the current trace represent 50-ms voltage pulses (in a compressed timescale) used to obtain the half-maximally activating concentration of K^+ (from Hill fits to the K^+ concentration dependence on outward currents). Application of 10 mM ouabain inhibits the K^+-induced outward Na/K pump current. B. Voltage dependence of $K_{0.5}$ for K^+ activation of outward pump currents at two extemal pHs (black: 7.6 and red: 9.6), in the presence (filled symbols, 125 mM external Na^+) and absence (open symbols, 125 mM N-methyl-D-glucamine (NMG)) of Na^+ in the external solution. Data points represent mean and standard deviation from five oocytes, for which titration at both pHs was evaluated. Figure was taken from Ref. [12]

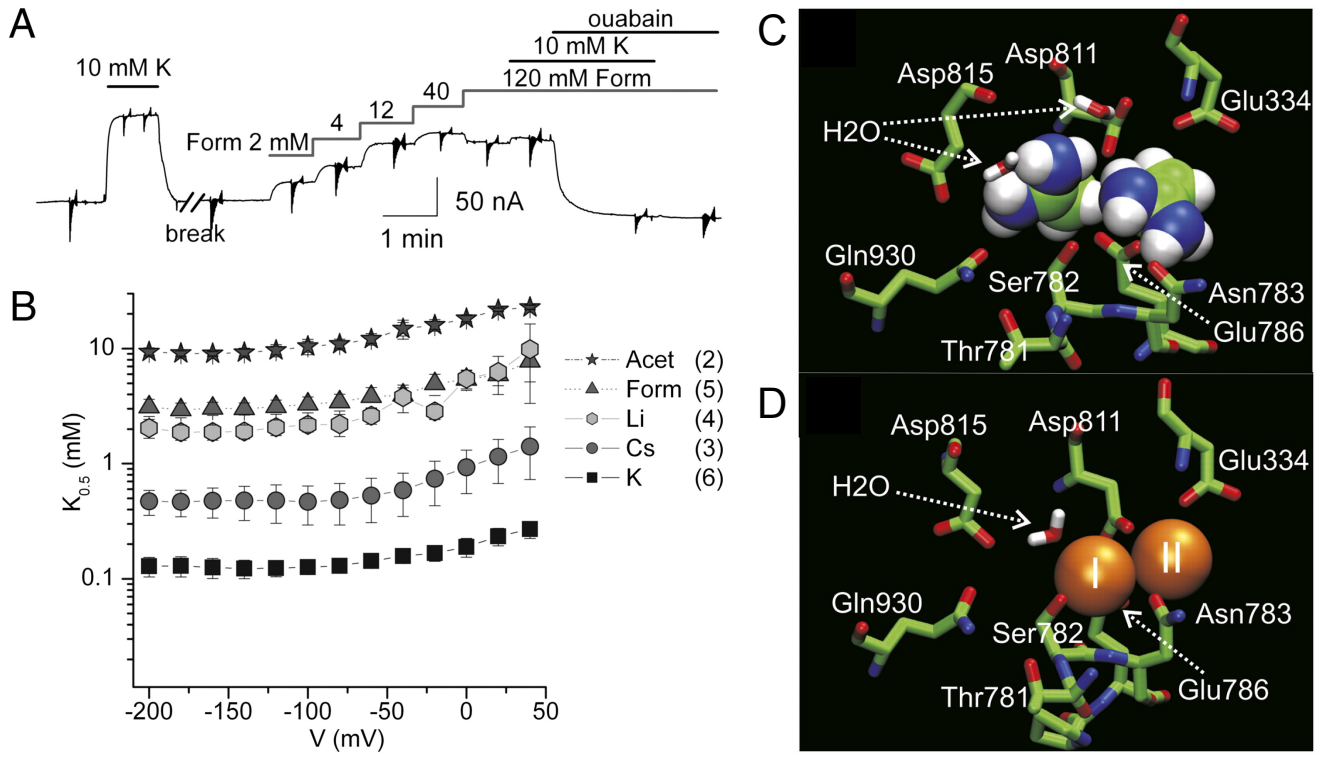

Figure 4: Electrophysiological experiments on the Na/K pump expressed in *Xenopus* oocytes with external surrogate alkali metals (Li^+ and Cs^+) and organic cations (Acet and Form). A. Cation activation of outward currents from a single Na^+-loaded oocyte held at -50 mV. Initial application of 10 mM K_0^+ (in NMG_0^+) gave an estimate of the maximal outward pump current. After K_0^+ washout, the oocyte was superfused with other external-cation solutions (Li^+, Cs^+, Acet, and Form). Shown after the break are step increments in [$Form_0^+$] (adjusting NMG_0^+ to achieve 120 mM) from 0 to 120 mM $Form_0^+$. Addition of 10 mM K_0^+ to the 120 mM $Form_0^+$ solution increased outward current only slightly. B. Voltage dependence of the half-maximal constant ($K_{0.5}$) for activation of outward current in the absence of external Na_0^+. Data points are means ± SEM of (n) experiments in different oocytes. C. Final configuration following a 20 ns equilibrium MD simulation started from a model of the complex with two Acet docked at the K^+ binding sites. D. Final configuration following a 20 ns equilibrium MD simulation of the crystallographic structure with K^+ ions bound (PDB id: 2ZXE[10]). Figure was adapted from Ref [13].

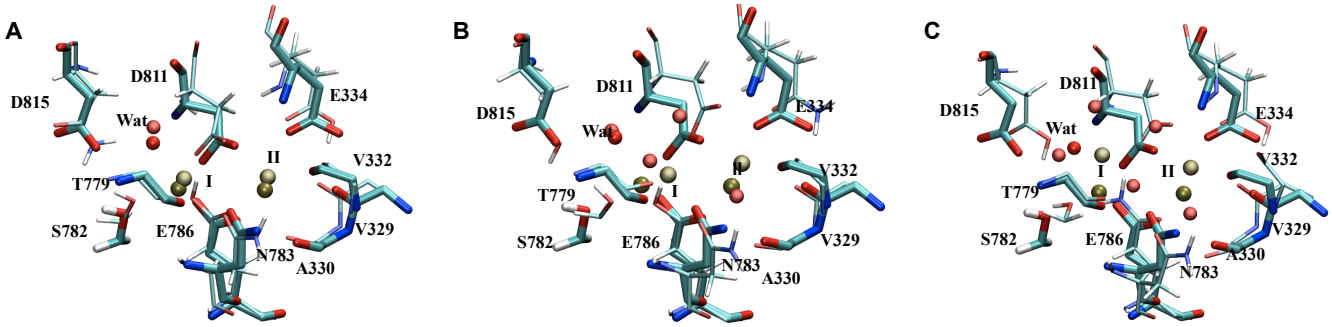

Figure 5: Final snapshots at 10 ns equilibrium simulations for the mutants (thin lines) superimposed with the crystal structure (thick lines, PDB id: 2ZXE[10]): A. D815N (Table 2 Simulation F); B. E334Q (Table 2 Simulation G); C. E786Q (Table 2 Simulation H). Figure was adapted from Supplementary Information in Ref [12].

REFERENCES:

[1] Glynn, I. M. A hundred years of sodium pumping *Annual review of physiology* 2002, *64*, 1.
[2] Clarke, R. J.; Fan, X. Pumping ions *Clinical and experimental pharmacology & physiology* 2011, *38*, 726.
[3] Palmgren, M. G.; Nissen, P. P-type ATPases *Annual review of biophysics* 2011, *40*, 243.
[4] Albers, R. W. Biochemical aspects of active transport *Annu Rev Biochem* 1967, *36*, 727.
[5] Post, R. L.; Hegyvary, C.; Kume, S. Activation by adenosine triphosphate in the phosphorylation kinetics of sodium and potassium ion transport adenosine triphosphatase *J Biol Chem* 1972, *247*, 6530.
[6] Prassas, I.; Diamandis, E. P. Novel therapeutic applications of cardiac glycosides *Nature reviews. Drug discovery* 2008, *7*, 926.
[7] Morth, J. P.; Pedersen, B. P.; Buch-Pedersen, M. J.; Andersen, J. P.; Vilsen, B.; Palmgren, M. G.; Nissen, P. A structural overview of the plasma membrane Na+,K+-ATPase and H +-ATPase ion pumps *Nat Rev Mol Cell Biol* 2011, *12*, 60.
[8] Toyoshima, C.; Kanai, R.; Cornelius, F. First Crystal Structures of Na(+),K(+)-ATPase: New Light on the Oldest Ion Pump *Structure* 2011, *19*, 1732.
[9] Morth, J. P.; Pedersen, B. P.; Toustrup-Jensen, M. S.; Sorensen, T. L.; Petersen, J.; Andersen, J. P.; Vilsen, B.; Nissen, P. Crystal structure of the sodium-potassium pump *Nature* 2007, *450*, 1043.
[10] Shinoda, T.; Ogawa, H.; Cornelius, F.; Toyoshima, C. Crystal structure of the sodium-potassium pump at 2.4 A resolution *Nature* 2009, *459*, 446.
[11] Ogawa, H.; Toyoshima, C. Homology modeling of the cation binding sites of Na+K+-ATPase *Proc. Natl. Acad. Sci. U. S. A.* 2002, *99*, 15977.
[12] Yu, H.; Ratheal, I. M.; Artigas, P.; Roux, B. Protonation of key acidic residues is critical for the K(+)-selectivity of the Na/K pump *Nat Struct Mol Biol* 2011, *18*, 1159.
[13] Ratheal, I. M.; Virgin, G. K.; Yu, H.; Roux, B.; Gatto, C.; Artigas, P. Selectivity of externally facing ion-binding sites in the Na/K pump to alkali metals and organic cations *Proc Natl Acad Sci U S A* 2010, *107*, 18718.
[14] Vrbka, L.; Vondrasek, J.; Jagoda-Cwiklik, B.; Vacha, R.; Jungwirth, P. Quantification and rationalization of the higher affinity of sodium over potassium to protein surfaces *Proc Natl Acad Sci U S A* 2006, *103*, 15440.
[15] Noskov, S. Y.; Roux, B. Control of ion selectivity in LeuT: two Na+ binding sites with two different mechanisms *J. Mol. Biol.* 2008, *377*, 804.
[16] Perrin, C. L.; Nielson, J. B. "Strong" hydrogen bonds in chemistry and biology *Annu Rev Phys Chem* 1997, *48*, 511.
[17] Phatak, P.; Ghosh, N.; Yu, H.; Cui, Q.; Elstner, M. Amino acids with an intermolecular proton bond as proton storage site in bacteriorhodopsin *Proc Natl Acad Sci U S A* 2008, *105*, 19672.
[18] Obara, K.; Miyashita, N.; Xu, C.; Toyoshima, I.; Sugita, Y.; Inesi, G.; Toyoshima, C. Structural role of countertransport revealed in Ca(2+) pump crystal structure in the absence of Ca(2+) *Proc Natl Acad Sci U S A* 2005, *102*, 14489.
[19] Sugita, Y.; Miyashita, N.; Ikeguchi, M.; Kidera, A.; Toyoshima, C. Protonation of the acidic residues in the transmembrane cation-binding sites of the ca(2+) pump *J Am Chem Soc* 2005, *127*, 6150.
[20] Hauser, K.; Barth, A. Side-chain protonation and mobility in the sarcoplasmic reticulum Ca2+-ATPase: implications for proton countertransport and Ca2+ release *Biophys J* 2007, *93*, 3259.

[21] Schmid, R.; Miah, A. M.; Sapunov, V. N. A new table of the thermodynamic quantities of ionic hydration: values and some applications (enthalpy-entropy compensation and Born radii) *Physical Chemistry Chemical Physics* 2000, *2*, 97.
[22] Lauger, P. *Electrogenic Ion Pumps*; 1st ed.; Sinauer Associates: Sunderland, Massachusetts, USA, 1991.
[23] Skou, J. C. Effects of ATP on the intermediary steps of the reaction of the (Na+ + K+)-ATPase. IV. Effect of ATP on K0.5 for Na+ and on hydrolysis at different pH and temperature *Biochim Biophys Acta* 1979, *567*, 421.
[24] Skou, J. C.; Esmann, M. Effects of ATP and protons on the Na : K selectivity of the (Na+ + K+)-ATPase studied by ligand effects on intrinsic and extrinsic fluorescence *Biochim Biophys Acta* 1980, *601*, 386.
[25] Breitwieser, G. E.; Altamirano, A. A.; Russell, J. M. Effects of pH changes on sodium pump fluxes in squid giant axon *The American journal of physiology* 1987, *253*, C547.
[26] Salonikidis, P. S.; Kirichenko, S. N.; Tatjanenko, L. V.; Schwarz, W.; Vasilets, L. A. Extracellular pH modulates kinetics of the Na(+),K(+)-ATPase *Biochim Biophys Acta* 2000, *1509*, 496.
[27] Milanick, M. A.; Arnett, K. L. Extracellular protons regulate the extracellular cation selectivity of the sodium pump *J Gen Physiol* 2002, *120*, 497.
[28] Yu, H.; Noskov, S. Y.; Roux, B. Two mechanisms of ion selectivity in protein binding sites *Proc. Natl. Acad. Sci. U. S. A.* 2010, *107*, 20329.
[29] Bezanilla, F.; Armstrong, C. M. Negative conductance caused by entry of sodium and cesium ions into the potassium channels of squid axons *J Gen Physiol* 1972, *60*, 588.
[30] Roux, B.; Berneche, S.; Egwolf, B.; Lev, B.; Noskov, S. Y.; Rowley, C. N.; Yu, H. Ion selectivity in channels and transporters *J Gen Physiol* 2011, *137*, 415.
[31] Noskov, S. Y.; Berneche, S.; Roux, B. Control of ion selectivity in potassium channels by electrostatic and dynamic properties of carbonyl ligands *Nature* 2004, *431*, 830.
[32] Noskov, S. Y.; Roux, B. Importance of hydration and dynamics on the selectivity of the KcsA and NaK channels *J Gen Physiol* 2007, *129*, 135.
[33] Kuntzweiler, T. A.; Wallick, E. T.; Johnson, C. L.; Lingrel, J. B. Glutamic acid 327 in the sheep alpha 1 isoform of Na+,K(+)-ATPase stabilizes a K(+)-induced conformational change *J Biol Chem* 1995, *270*, 2993.
[34] Koenderink, J. B.; Geibel, S.; Grabsch, E.; De Pont, J. J.; Bamberg, E.; Friedrich, T. Electrophysiological analysis of the mutated Na,K-ATPase cation binding pocket *J Biol Chem* 2003, *278*, 51213.
[35] Toyoshima, C. Structural aspects of ion pumping by Ca2+-ATPase of sarcoplasmic reticulum *Arch Biochem Biophys* 2008, *476*, 3.
[36] Andersson, J.; Hauser, K.; Karjalainen, E. L.; Barth, A. Protonation and hydrogen bonding of Ca2+ site residues in the E2P phosphoenzyme intermediate of sarcoplasmic reticulum Ca2+-ATPase studied by a combination of infrared spectroscopy and electrostatic calculations *Biophys J* 2008, *94*, 600.
[37] Weidemuller, C.; Hauser, K. Ion transport and energy transduction of P-type ATPases: implications from electrostatic calculations *Biochim Biophys Acta* 2009, *1787*, 721.
[38] Musgaard, M.; Thogersen, L.; Schiott, B. Protonation States of Important Acidic Residues in the Central Ca(2+) Ion Binding Sites of the Ca(2+)-ATPase: A Molecular Modeling Study *Biochemistry* 2011, *50*, 11109.
[39] Bublitz, M.; Poulsen, H.; Morth, J. P.; Nissen, P. In and out of the cation pumps: P-type ATPase structure revisited *Curr Opin Struct Biol* 2010, *20*, 431.
[40] Poulsen, H.; Khandelia, H.; Morth, J. P.; Bublitz, M.; Mouritsen, O. G.; Egebjerg, J.; Nissen, P. Neurological disease mutations compromise a C-terminal ion pathway in the Na(+)/K(+)-ATPase *Nature* 2010, *467*, 99.

[41] Roux, B. Exploring the ion selectivity properties of a large number of simplified binding site models *Biophys J* 2010, *98*, 2877.
[42] Thompson, A. N.; Kim, I.; Panosian, T. D.; Iverson, T. M.; Allen, T. W.; Nimigean, C. M. Mechanism of potassium-channel selectivity revealed by Na(+) and Li(+) binding sites within the KcsA pore *Nat Struct Mol Biol* 2009, *16*, 1317.
[43] Myers, S. L.; Cornelius, F.; Apell, H. J.; Clarke, R. J. Kinetics of K(+) occlusion by the phosphoenzyme of the Na(+),K(+)-ATPase *Biophys J* 2011, *100*, 70.
[44] van Gunsteren, W. F.; Mark, A. E. Validation of molecular dynamics simulation *J Chem Phys* 1998, *108*, 6109.
[45] van Gunsteren, W. F.; Bakowies, D.; Baron, R.; Chandrasekhar, I.; Christen, M.; Daura, X.; Gee, P.; Geerke, D. P.; Glattli, A.; Hunenberger, P. H.; Kastenholz, M. A.; Ostenbrink, C.; Schenk, M.; Trzesniak, D.; van der Vegt, N. F. A.; Yu, H. B. Biomolecular modeling: Goals, problems, perspectives *Angew Chem Int Edit* 2006, *45*, 4064.
[46] Oostenbrink, C.; Villa, A.; Mark, A. E.; Van Gunsteren, W. F. A biomolecular force field based on the free enthalpy of hydration and solvation: The GROMOS force-field parameter sets 53A5 and 53A6 *J Comput Chem* 2004, *25*, 1656.
[47] Cornell, W. D.; Cieplak, P.; Bayly, C. I.; Gould, I. R.; Merz, K. M.; Ferguson, D. M.; Spellmeyer, D. C.; Fox, T.; Caldwell, J. W.; Kollman, P. A. A Second Generation Force Field for the Simulation of Proteins, Nucleic Acids, and Organic Molecules *J. Am. Chem. Soc.* 1995, *117*, 5179.
[48] MacKerell, A. D.; Bashford, D.; Bellott; Dunbrack, R. L.; Evanseck, J. D.; Field, M. J.; Fischer, S.; Gao, J.; Guo, H.; Ha, S.; Joseph-McCarthy, D.; Kuchnir, L.; Kuczera, K.; Lau, F. T. K.; Mattos, C.; Michnick, S.; Ngo, T.; Nguyen, D. T.; Prodhom, B.; Reiher, W. E.; Roux, B.; Schlenkrich, M.; Smith, J. C.; Stote, R.; Straub, J.; Watanabe, M.; Wiórkiewicz-Kuczera, J.; Yin, D.; Karplus, M. All-Atom Empirical Potential for Molecular Modeling and Dynamics Studies of Proteins† *The Journal of Physical Chemistry B* 1998, *102*, 3586.
[49] Bucher, D.; Rothlisberger, U. Molecular simulations of ion channels: a quantum chemist's perspective *J Gen Physiol* 2010, *135*, 549.
[50] Bucher, D.; Guidoni, L.; Carloni, P.; Rothlisberger, U. Coordination numbers of K(+) and Na(+) Ions inside the selectivity filter of the KcsA potassium channel: insights from first principles molecular dynamics *Biophys J* 2010, *98*, L47.
[51] Bucher, D.; Raugei, S.; Guidoni, L.; Dal Peraro, M.; Rothlisberger, U.; Carloni, P.; Klein, M. L. Polarization effects and charge transfer in the KcsA potassium channel *Biophys Chem* 2006, *124*, 292.
[52] Timko, J.; Bucher, D.; Kuyucak, S. Dissociation of NaCl in water from ab initio molecular dynamics simulations *J Chem Phys* 2010, *132*, 114510.
[53] Yu, H. B.; van Gunsteren, W. F. Accounting for polarization in molecular simulation *Comput Phys Commun* 2005, *172*, 69.
[54] Lopes, P. E.; Roux, B.; Mackerell, A. D., Jr. Molecular modeling and dynamics studies with explicit inclusion of electronic polarizability. Theory and applications *Theor Chem Acc* 2009, *124*, 11.
[55] Ponder, J. W.; Wu, C.; Ren, P.; Pande, V. S.; Chodera, J. D.; Schnieders, M. J.; Haque, I.; Mobley, D. L.; Lambrecht, D. S.; DiStasio, R. A., Jr.; Head-Gordon, M.; Clark, G. N.; Johnson, M. E.; Head-Gordon, T. Current status of the AMOEBA polarizable force field *J Phys Chem B* 2010, *114*, 2549.
[56] Warshel, A.; Kato, M.; Pisliakov, A. V. Polarizable Force Fields: History, Test Cases, and Prospects *J Chem Theory Comput* 2007, *3*, 2034.

[57] Yu, H. B.; Mazzanti, C. L.; Whitfield, T. W.; Koeppe, R. E.; Andersen, O. S.; Roux, B. A combined experimental and theoretical study of ion solvation in liquid N-methylacetamide *J Am Chem Soc* 2010, *132*, 10847.
[58] Yu, H.; Whitfield, T. W.; Harder, E.; Lamoureux, G.; Vorobyov, I.; Anisimov, V. M.; Mackerell, A. D., Jr.; Roux, B. Simulating Monovalent and Divalent Ions in Aqueous Solution Using a Drude Polarizable Force Field *J Chem Theory Comput* 2010, *6*, 774.
[59] Georgescu, R. E.; Alexov, E. G.; Gunner, M. R. Combining conformational flexibility and continuum electrostatics for calculating pK(a)s in proteins *Biophys J* 2002, *83*, 1731.
[60] Song, Y.; Mao, J.; Gunner, M. R. MCCE2: improving protein pKa calculations with extensive side chain rotamer sampling *J Comput Chem* 2009, *30*, 2231.
[61] Li, H.; Robertson, A. D.; Jensen, J. H. Very fast empirical prediction and rationalization of protein pKa values *Proteins* 2005, *61*, 704.